MANCHESTER 1824
The University of Manchester

The University of Manchester Research

Mitigating stochastic uncertainty from weather routing for ships with wind propulsion

DOI:
10.1016/j.oceaneng.2023.114674

Document Version
Final published version

Link to publication record in Manchester Research Explorer

Citation for published version (APA):
Mason, J., Larkin, A., & Gallego-Schmid, A. (2023). Mitigating stochastic uncertainty from weather routing for ships with wind propulsion. *Ocean Engineering*, *281*, [114674]. https://doi.org/10.1016/j.oceaneng.2023.114674

Published in:
Ocean Engineering

Citing this paper
Please note that where the full-text provided on Manchester Research Explorer is the Author Accepted Manuscript or Proof version this may differ from the final Published version. If citing, it is advised that you check and use the publisher's definitive version.

General rights
Copyright and moral rights for the publications made accessible in the Research Explorer are retained by the authors and/or other copyright owners and it is a condition of accessing publications that users recognise and abide by the legal requirements associated with these rights.

Takedown policy
If you believe that this document breaches copyright please refer to the University of Manchester's Takedown Procedures [http://man.ac.uk/04Y6Bo] or contact uml.scholarlycommunications@manchester.ac.uk providing relevant details, so we can investigate your claim.

Download date:18. Jul. 2023

Ocean Engineering 281 (2023) 114674

Contents lists available at ScienceDirect

Ocean Engineering

journal homepage: www.elsevier.com/locate/oceaneng

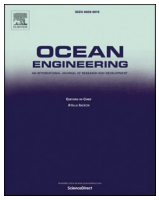

Mitigating stochastic uncertainty from weather routing for ships with wind propulsion

James Mason *, Alice Larkin, Alejandro Gallego-Schmid **

Tyndall Centre for Climate Change Research, Department of Mechanical, Aerospace and Civil Engineering, Faculty of Science and Engineering, The University of Manchester, M13 9PL, Manchester, United Kingdom

ARTICLE INFO

Handling Editor: Prof. A.I. Incecik

Keywords:
Weather routing
Wind propulsion
Flettner rotors
Optimisation
Climate change
Carbon savings

ABSTRACT

Reducing the shipping sector's contribution to climate change requires urgent emission reductions this decade. Both weather routing and wind propulsion offer immediate solutions, where combining sails with efficient routing amplifies the performance of each technology. However, while large emission savings are theoretically available, the impact of stochastic uncertainty from wind forecasts is unknown. Here, we present a novel approach that exploits fuel consumption calculations from over a thousand departures across three routes to characterise stochastic uncertainty. We show that routes with ideal wind conditions and long voyage times are most sensitive to uncertain forecast inputs, reducing savings from Flettner rotors and weather routing by up to 44% when a priori weather routing strategies are used. This paper further shows how an adaptive weather routing strategy can be used as an accurate prediction tool to reduce uncertainty on all routes investigated, reliably amplifying carbon savings from Flettner rotors by between 1.16 and 2.48 times typical great circle route savings. Overall, this paper provides greater assurance around the previously estimated carbon savings that serves to strengthen confidence in a wind-assisted decarbonisation strategy and its potential to provide essential emission reductions this decade.

1. Introduction

The climate emergency requires all sectors to urgently reduce their carbon emissions to avoid dangerous levels of climate change. The international shipping sector contributes to 2–3% of global carbon emissions annually (IMO, 2020) and existing industry targets aim to cut carbon by 50% relative to 2008 levels by 2050 (IMO, 2018). Studies show that this target falls short of the deep and urgent cuts required to avoid a 1.5 °C global temperature rise in line with the Paris Climate Agreement. According to Bullock et al. (2022), the sector must accelerate its ambition and shift focus towards urgent short-term action to cut CO_2 by 34% by 2030 with full decarbonisation by 2050. Moreover, the existing shipping fleet could consume 135% of a 1.5 °C Paris compatible carbon budget if the sector implements no mitigation measures, as the long lifetime of ships commits the industry to carbon emissions for decades into the future (Bullock et al., 2020). Urgent action that targets retrofit technologies on existing ships is therefore an essential component of a Paris-aligned emission trajectory for international shipping.

Wind propulsion technology aligns with this short-term focus, where sails such as Flettner rotors, wing sails and suction wings produce direct energy from the wind to reduce the power consumed by a ship's engine. Over twenty installations across the last decade show emerging interest in the technology as stakeholders in the sector attempt to decarbonise and reduce operational expenditure (IMO, 2022). While wind propulsion could generate some of the urgent short-term carbon savings needed to keep the sector within the scientific interpretation of the Paris Climate Agreement, the technology also reduces the long-term risk posed by uncertain low-carbon shipping fuels and could partially shield ship owners from risks such as fuel cost volatility and bunkering availability (Ampah et al., 2021). Furthermore, ship owners can install wind propulsion to meet the sector's energy efficiency existing index (EEXI) and the carbon intensity indicator (CII) target introduced in 2023, to combat rising emissions in the sector.

Studies demonstrate a synergistic benefit from combining wind propulsion technology with weather routing software (Marie and Courteille, 2014; Mason, 2021). Weather routing facilitates greater carbon savings from wind propulsion by allowing a ship to deviate from standard shipping routes to search for advantageous wind profiles.

* Corresponding author.
** Corresponding author.
E-mail addresses: james.mason@manchester.ac.uk (J. Mason), alejandro.gallegoschmid@manchester.ac.uk (A. Gallego-Schmid).

https://doi.org/10.1016/j.oceaneng.2023.114674
Received 20 December 2022; Received in revised form 14 April 2023; Accepted 23 April 2023
Available online 8 May 2023
0029-8018/© 2023 The Authors. Published by Elsevier Ltd. This is an open access article under the CC BY license (http://creativecommons.org/licenses/by/4.0/).

Mason (2021) shows that weather routing can substantially increase the carbon savings from a wind-assisted Panamax bulk carrier to over 30% on particularly favourable routes. While such large carbon savings would likely be very attractive to the shipping sector if realised in practice, theoretical savings may differ from reality due to idealised parameters assumed within weather routing methods in the literature. Studies optimise shipping routes using idealised reanalysis wind data (Zhang et al., 2013; Bentin et al., 2016), which assumes a perfect historical foresight of future weather. While this is useful to understand the maximum benefits available from the technology, only wind forecast data is available to ships operating in real-time, which introduces uncertainties.

All studies that integrate wind forecast data to calculate weather routing use a priori optimisation strategies (Ueno et al., 2004; Marie and Courteille, 2014; Yoshimura et al., 2016). In vehicle routing problems, a priori strategies use information that is available at the start of the journey only (Manseur et al., 2018). For ships, this involves utilising the weather forecast that is available to the ship as it departs. While a priori methods are not used in practice, they are useful in theory to estimate the potential benefits of weather routing. However, a priori methods are limited, as wind conditions could deviate from the forecast as the ship moves along its journey due to stochastic uncertainty. Wind that deviates from the initial forecast prediction could detrimentally reduce the carbon savings from weather routing as the ship travels along an uncertain optimum route. There remains a knowledge gap around the sensitivity of a priori weather routing to wind forecast data in existing scientific studies.

In this regard, Yoshimura et al. (2016) investigate how forecast uncertainties impact ships with wind propulsion when using a priori weather routing strategies. By using 21 ensemble forecast members on a case study departure in the Pacific Ocean, the authors demonstrate that stochastic wind forecasts can generate substantial uncertainty, as fuel savings vary from 32% to 92%. Moreover, Rosander and Bloch (2000) show that stochastic uncertainty removes all benefits from weather routing when a priori optimum routes are sailed in practice. However, wind conditions vary over different departure dates and studies are yet to quantify a statistically robust estimate of stochastic uncertainty across many departures. Furthermore, the variability of wind conditions changes on routes around the globe and for different route lengths. However, no study yet links route attributes to stochastic uncertainty to characterise which routes are most affected by forecast uncertainty and why. Understanding these dominant attributes would provide a deeper understanding of which routes may require more detailed methods than a priori strategies to provide accurate estimations in future studies.

The analysis in this paper develops an a priori optimisation strategy to investigate how stochastic uncertainty impacts methods in the existing scientific literature. For 1080 departures across the eastbound and westbound journeys relating to three case study routes in the North Sea, South Atlantic Ocean and North Atlantic Ocean, the optimum shipping voyage is calculated using a priori forecast data. The resulting optimum route is then retracked with historical data to calculate the savings that would be realised from this strategy in practice by operating ships. By simulating over 1000 departures, this novel approach extends the work of Rosander and Bloch (2000) and Yoshimura et al. (2016), which simulate only a handful of departures, to provide the first statistically robust estimates of a priori weather routing. This approach deepens the understanding of how theoretical savings presented in the scientific literature would play out in practice on average over a year. Furthermore, fuel consumption data is correlated with route attributes to provide the first characterisation in the literature on which routes are most sensitive to stochastic uncertainty when using wind propulsion and why. Ultimately, this new approach identifies which routes require modelling with methods that more accurately reflect industry practices to investigate whether the theoretical savings presented in the literature are achievable in practice, or whether they represent idealised values.

Finally, while methods exist to reduce uncertainty in the wider field of ship and vehicle routing problems (Hinnethal and Clauss, 2010; Deyemer et al., 2013; Vettor et al., 2021), Rosander and Bloch (2000) develop the only method to reduce uncertainty for ships with wind propulsion by producing an adaptive weather routing strategy. The adaptive method mirrors standard routing procedures in the shipping industry, where the routing system uploads new weather forecast data every 24 h and reruns the weather routing procedure to reduce uncertainty. Unlike a priori methods, adaptive strategies reflect practices used in the industry and results from this method more reliably depict the carbon savings available from weather routing in practice. Rosander and Bloch (2000) find that stochastic uncertainty removes all benefits from weather routing when optimal adaptive routes are sailed in practice. While this result highlights potential limitations in the applicability of standard shipping practices, weather forecast predictions have improved in accuracy since this study and the impact of these advances is unknown. To understand how advances in wind forecast predictions affect the results presented in Rosander and Bloch (2000), this study additionally develops an adaptive optimisation strategy that incorporates the latest wind forecast prediction data across a wider range of departures. By updating wind forecast data every 12 h to recursively acquire the most accurate forecast data available, the analysis deepens the understanding of whether existing weather routing practices in the sector are suitable to reduce the risk from stochastic wind forecasts, and whether existing practices can achieve the theoretical carbon savings presented by a priori estimates in the existing scientific literature. Overall, these results update and extend the work from Rosander and Bloch (2000) to provide further insights into the scale of carbon reductions available from wind propulsion when coupled with weather routing and how these solutions can combine to form a short-term decarbonisation strategy for shipping that provides the best chance of aligning emissions trajectories with Paris-compliant goals.

This article is divided into seven main parts. Section 2 outlines the wind-assisted ship propulsion (WASP) model that is used to calculate the performance of a wind-assisted ship with four Flettner rotors installed. Section 3 describes the ship routing model that calculates carbon emissions on the great circle route and the optimised voyage with weather routing. Section 4 discusses the three case study routes that this study simulates. Sections 5 and 6 discuss the results of the a priori and adaptive strategies. Section 7 highlights the limitations of the study, and finally, Section 8 presents the conclusions.

2. The wind-assisted ship propulsion (WASP) model

This study uses a wind-assisted ship propulsion (WASP) model sourced through a collaboration with Delft University of Technology. The model is developed independently of the work carried out in this analysis and a full description can be found in Bordogna et al. (2019), van der Kolk et al. (2019), Bordogna et al. (2020) and van der Kolk et al. (2020).

The WASP model calculates the fuel consumption of an 80,000 DWT Panamax bulk carrier ship with four Flettner rotors installed. Each rotor has a height of 35 m and a diameter of 5 m, matching the maximum size of Flettner rotors currently available. The ship has a design speed of 14.5 knots and a fully loaded draft of 14 m. Panamax bulk carrier ships represent ideal candidates for wind propulsion technology due to their ample deck space, and the Panamax fleet contributed to around 6% of the shipping sector's carbon emissions in 2018 (IMO, 2020).

The model calculates forces acting on the wind-assisted ship in four degrees of motion to estimate the power required by the engine to maintain a predefined ship speed. The ship is assumed to be in fully laden condition. The model is split into two parts: aerodynamic modelling and hydrodynamic modelling. Aerodynamic modelling computes the forces produced by the Flettner rotor sails. Results from wind tunnel experiments are used to validate a mathematical model that calculates the lift, drag and heel forces produced by the Flettner rotors, and interactions between multiple Flettner rotors and wind perturbation

effects from the ship's hull are included (Bordogna et al., 2019, 2020). Additionally, the rotation speed of the Flettner rotors is configured to provide the maximum forward thrust for each wind speed and wind angle, which allows the system to turn off in strong headwinds to mitigate detrimental forces. Hydrodynamic modelling uses full-scale simulation data from the Delft Wind Assist series to calculate the resistance of the ship. Modelling includes the added resistance induced by the heel and leeway angles, which are created by the additional Flettner rotor forces. Hulls of this data series are analysed using a Reynolds-Averages Navier Stokes computational fluid dynamics (RANS-CFD) method (van der Kolk et al., 2019, 2020). An increased rudder angle is modelled to counteract the ship's oblique motion through the water and a maximum limit of ten degrees is set to ensure the ship can suitably operate.

The power from the Flettner rotors, $F_{Flettner}$, and the resulting ship resistance $F_{resistance}$, are used to calculate the engine power of the ship using:

$$P_B = \left(\frac{v_{ship}}{\eta_T} (F_{resistance} - F_{Flettner}) + \frac{P_{input}}{\eta_{Gen}} \right) \quad (1)$$

Here, v_{ship} is the ship's speed and P_{input} is the power required to spin the Flettner rotors. η_T represents efficiency losses from the ship's drive train and propeller and is set here as 0.7 as suggested by IMO guidance documents (IMO, 2021), while η_{Gen} represents the conversion efficiency to power the Flettner rotors and is set here as 0.85 (Smith et al., 2013). Finally, engine power is converted to fuel consumption by multiplying by a variable specific fuel consumption (SFC) defined in IMO (2014). The performance polar diagrams for the wind-assisted Panamax bulk carrier can be found in Supplementary Fig. 1 for ship speeds between 8 and 14 knots.

Added resistance in waves is calculated using the Gerritsma-Beukelman method (Gerritsma and Beukelman, 1972), which has been shown to be a good approximation (Lu et al., 2015; Kim et al., 2017). Wave direction is assumed to coincide with wind direction, and the wave height is calculated using the Pierson-Moskowitz method (Pierson and Moskowitz, 1964). While the Gerritsma-Beukelman method can underestimate ship resistance in the short-wave region, this study calculates the performance of both a wind-assisted ship and a standard ship with no sails using this method. Here we calculate the percentage carbon savings between these two ship types to reduce the impact of this error.

3. Ship routing

This study develops a ship routing model to quantify the impact of stochastic wind forecasts on weather routing for ships with wind propulsion. An overview of the model is shown in Fig. 1. The model can be broken down into the following steps.

1. Load simulation inputs for route and departure date.
2. Create graphs for the optimisation procedure.
3. Run great circle route and weather routing simulations, including a priori and adaptive strategy simulations.
4. Calculate carbon savings and other performance indicators.

This section describes the method that is used to calculate ship routing in steps 2–4 of the model, including great circle routing and weather routing. Further details on the simulation inputs in Step 1 can be found in the case study descriptions in Section 4.

3.1. Great circle route

Automatic identification system (AIS) ship routing data is used here to represent the typical great circle route of three case study routes. The data consists of both the positional points (longitude and latitude) and the speed over ground of the ship. The fuel consumption between adjacent positional points, defined here as a stage, is then calculated through the following steps.

First, the ship bearing is calculated for each stage of the route and is

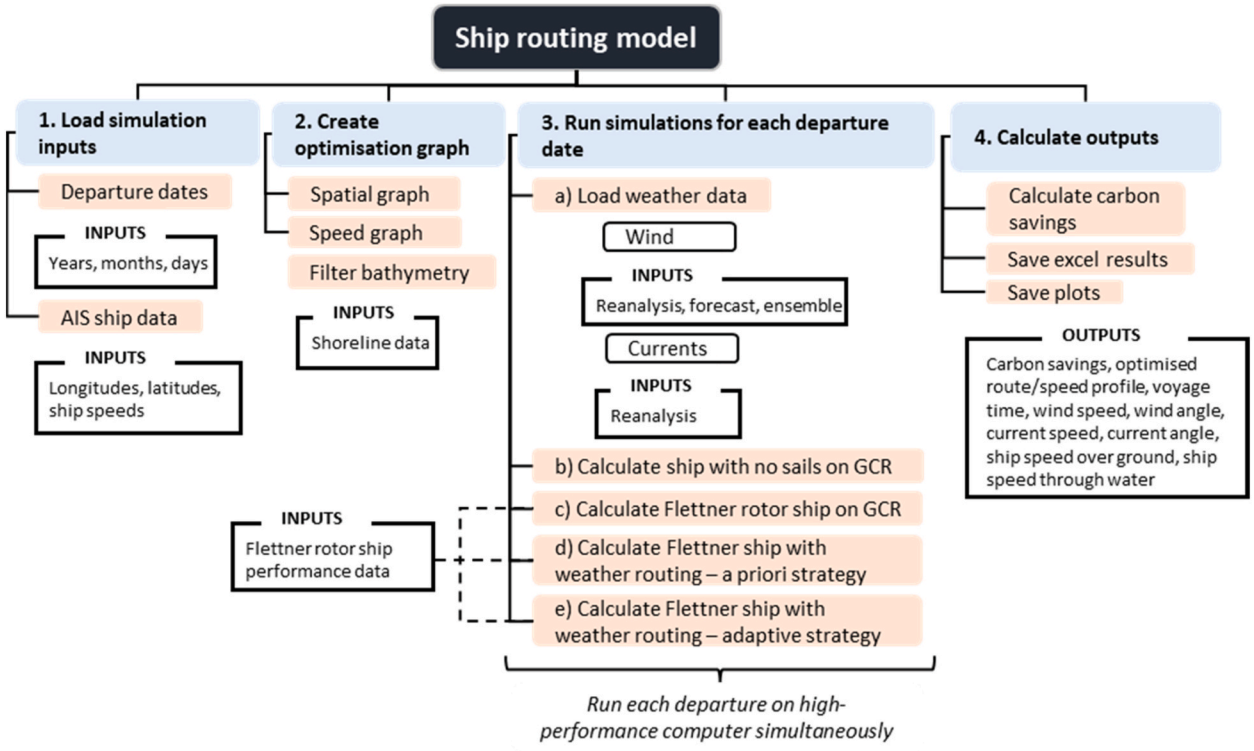

Fig. 1. An overview of the weather routing method used in this study.

combined with ocean current data to calculate the ship's speed through water. Here, ocean current data is obtained from the Earth Space Research's (ESR) Ocean Surface Current Analysis Real-time (OSCAR) dataset (ESR, 2009), which contains reanalysis current data with a third-degree spatial resolution and a 5-day time resolution. Historical reanalysis ocean current data is used here, which assumes the ocean current is known exactly with no uncertainty, as ocean current forecast data is more stable than wind forecast data and exhibits less stochastic uncertainty (Kristensen, 2010). At each stage, the true ocean current speed (TCS) and true ocean current angle (TCA) are calculated, and the ship's bearing is used to determine the ocean current speed in the direction of motion of the ship. The ocean current speed in the direction of motion of the ship is then combined with the ship's speed over ground to calculate the speed through water at each stage.

Finally, wind data is loaded into the model, which is used alongside the ship's speed through water as inputs into the WASP model to calculate the fuel consumption of the ship along the route. Here, reanalysis wind data is obtained from the European Centre for Medium-range Weather Forecasts (ECMWF) ERA5 dataset with a 0.5-degree spatial resolution and a 6-h time resolution (ECMWF, 2022). At each stage, the true wind speed (TWS) and true wind angle (TWA) are calculated, and the ship's bearing and speed over ground are used to calculate the apparent wind speed (AWS) and apparent wind angle (AWA). The WASP model then uses these inputs to calculate the fuel consumption of the ship at the specified speed through water for each stage. The fuel consumption along each stage is then summed to calculate the total fuel consumed along the journey. Here, the model calculates the fuel consumption of the reference ship and the wind-assisted ship, and the carbon savings, ΔE, are calculated using:

$$\Delta E = \frac{FC_R - FC_{WA}}{FC_R} \tag{2}$$

where FC represents fuel consumption, R represents the reference ship and WA represents the wind-assisted ship.

3.2. The voyage optimisation for the international decarbonisation of ships (VOIDS) weather routing model

In the face of the imminent climate crisis, weather routing technology represents an operational solution that enables ship operators to reduce their carbon emissions by optimising their route and speed profile along a journey. Weather routing can also amplify the carbon savings of wind propulsion technology, as optimal routing facilitates beneficial wind speeds and wind angles to produce synergistic benefits. The analysis in this study uses the VOIDS weather routing model, developed and presented for the first time in Mason (2021), to calculate the carbon savings from weather routing technology. This section discusses the method used to develop the VOIDS weather routing model.

3.2.1. Spatial optimisation graph

The VOIDS model uses a graph-based approach to optimise the route and speed of a ship on a route. To do this, first, a spatial optimisation graph and a ship speed-based graph are created (step 2 in the model outline of Fig. 1).

The spatial graph is created by transforming the great circle route to create a stage-based search space (Fig. 2a), which allows the optimisation to search over many possible combinations of routes. At each great circle point, new waypoints are created perpendicular to the direction of motion of the ship using lines of constant bearing, known as 'rhumb lines', using the method outlined in Morgas and Kopacz (2013). The great circle route and rhumb line points combine to form the nodes of the spatial optimisation graph. Movement is allowed between the nearest seven neighbouring nodes on the next stage by setting a maximum travel distance limit.

3.2.2. Ship speed graph

A ship speed-based graph is then created by predefining all possible ship speeds (Fig. 2b). The Panamax bulk carrier fleet had an average shipping speed of 12 knots between 2012 and 2018 (IMO, 2020) with the majority of the operating speed profiles falling in the 8 to 14 knots region (DNV GL, 2018). Therefore, this study sets possible ship speeds between 8 and 14 knots in 0.5-knot intervals. The ship can change its speed between each stage of the route to all other possible speeds. This forms thirteen neighbouring nodes on the speed-based graph. While ships typically sail at a constant engine power when travelling at sea, this study sets a constant speed between each stage, which aligns with many studies within the wind propulsion literature (Traut et al., 2014; Bentin et al., 2016; Seddiek and Ammar, 2021). A case study analysis by Wang et al. (2017) concludes that there are no significant differences between each method when they calculate optimal fuel savings for a ship without wind propulsion.

The positional and speed-based graphs combine to form a three-dimensional graph, G, with n vertices and a maximum of 91 neighbouring nodes between each stage. The weights, w, along the edges of

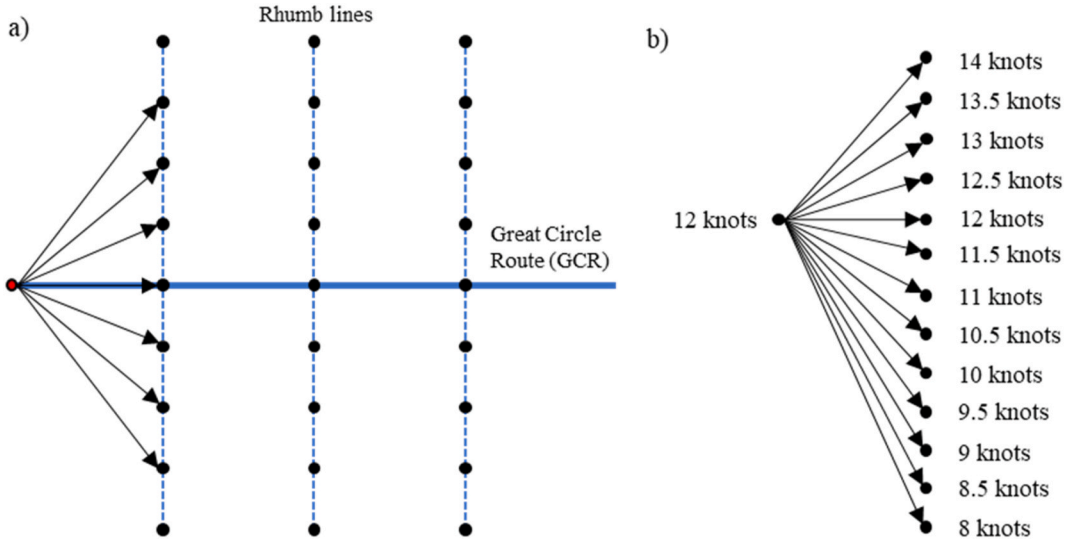

Fig. 2. The spatial graph (a) and the speed-based graph (b) used with the dynamic programming algorithm.

the graph that connect node i with neighbouring node j are set as the fuel consumption, FC, of the ship between the position of the two nodes (x_i, y_i) and (x_j, y_j), at a given ship speed v_{ship}, where:

$$w_{ij} = FC(x_i, y_i, x_j, y_j, v_{ship}) \tag{3}$$

$$FC(x_i, y_i, x_j, y_j, v_{ship}) = FC_{rate}(P_B) * \frac{d(x_i, y_i, x_j, y_j)}{v_{ship}} \tag{4}$$

Here, $FC_{rate}(P_B)$ is the rate of fuel consumption of the ship at a given ship speed, which is dependent on engine power (Equation (1)) and measured in kilograms of fuel per hour, and $d(x_i, y_i, x_j, y_j)$ is the distance between the positional points of node i and node j. Fuel consumption is used as the value along the graph's edges to ensure that minimum fuel consumption is calculated as the optimisation objective.

3.2.3. Three-dimensional dynamic programming

The VOIDS model uses a three-dimensional dynamic programming algorithm to calculate the optimum voyage of the ship and optimises fuel consumption as the single optimisation objective. While many weather routing studies optimise two or more objectives, including voyage time and passenger comfort, this study solely targets fuel consumption to reduce carbon emissions in the face of the imminent climate crisis. A time constraint equal to existing shipping practices is included, which ensures no detrimental impacts to supply chains.

Dynamic programming is a graph-based algorithm that uses Bellman's principle of optimality to find an optimum solution (Bellman, 1957). The algorithm is three-dimensional and incorporates three optimisation variables to find a fuel-optimum voyage: the position ((i) latitude and (ii) longitude) and (iii) speed profile of the ship. The algorithm calculates an optimum ship route and speed profile by searching across all possible solutions within the optimisation graph's search space. At the start node, the ship travels along the edges of the graph to all neighbouring nodes on the next stage, which includes the seven closest spatial points (Fig. 2a) and all speeds from 8 to 14 knots (Fig. 2b). The fuel consumption of the ship is calculated and stored. Once complete, each arrival point becomes the new departure point, and the ship again travels along the edges of the graph to all neighbouring nodes on the next stage. This process repeats until the destination of the ship is reached and the optimised voyage is selected as the route with the lowest fuel consumption. Finally, this fuel-optimal voyage is retracked using a retracking algorithm to obtain the route and speed profile of the ship along the voyage. Pseudocode for the algorithm is shown in Algorithm 1.

3.2.4. Local optimisation strategy

As dynamic programming is a graph-based algorithm, the computation time increases exponentially with the size of the graph. To reduce computation time, here we implement a local optimisation strategy. During the optimisation procedure, the ship will arrive at the same positional node with many possible previous route and speed combinations. Some of these potential voyages will arrive at the same time, but the ship will have consumed different volumes of fuel. In this study, if the ship arrives at the same positional node with the same arrival time, then only the voyage with the lowest fuel consumption is stored in memory. This requires the VOIDS model to round the arrival time of the ship. Rounding the arrival time to reduce the granularity of stored results leads to fewer potential routes stored in memory, subsequently reducing the computation time of the optimisation algorithm. Here, the local optimisation strategy is set to increments that allow the algorithm to run within a computation time of approximately 15 min for each simulation.

Algorithm 1. Three-dimensional dynamic programming algorithm

Algorithm 1: Three-dimensional dynamic programming algorithm

input : Spatial graph (G), set of spatial vertices (V), speed graph (P), set of speed vertices (X), source vertex (s), queue array (R), stage array (A), fuel consumption cost (FC), cost of edge from spatial position u to spatial position v at speed p (FC(u,v,p)), ETA limit (T), voyage time (t)

output: Optimised path and speed profile between the start and end vertices

```
FC(s) = 0 // Set FC at start vertex, s, to zero
R = {} // set up empty queue array holding visited elements
// Iterate over all stages in stage array, A
for all i ∈ A do
    // For each spatial vertex, u, in all vertices, V, from graph, G
    for all u ∈ V in graph G do
        // Find if the spatial vertex, u, is in the current stage, i, and hasn't already been visited
        Select u ∈ V with stage = i and u ∉ R
        R = R∪{u} // add u to the queue array
        // For all neighbouring spatial vertices, v, to spatial vertex, u
        for all v ∈ neighbours[u] do
            // For all neighbouring speed vertices, p, in all vertices, X, from graph, P
            for all p ∈ X in graph P do
                // If the new fuel consumption is less than the old fuel consumption, replace
                if FC(u) > FC(u) + FC(u,v,p) and t < T then
                    FC(v) = FC(u) + FC(u,v,p)
    Append(R,u)
```

3.3. Model constraints

Nodes on the spatial graph are filtered using bathymetry data from the General Bathymetric Chart of the Oceans (GEBCO) assuming a ship draught of 14 m (GEBCO, 2022). The filter reduces the size of the spatial graph and removes positional nodes that are either too shallow or land points (Fig. 3a). Similarly, during the optimisation procedure, the VOIDS model performs a land avoidance check to ensure that no land masses are crossed when the ship travels between any two neighbouring positional nodes. The land avoidance check uses shoreline data from the Global Self-consistent, Hierarchical, High-resolution Geography (GSHHG) database (NOAA, 2017).

When performing weather routing, the VOIDS model also sets an estimated time of arrival limit that is equal to the great circle route sailing time. This arrival time limit allows the optimised voyage to arrive at its destination with no delay. However, this practice can lead to ships spending a significant amount of time in port queues waiting to access a terminal. Bulk carriers spend around 9% of their time at anchorage (Merkel et al., 2022) and large carbon savings could be realised if ships spend this time slow steaming. While this is outside of the scope of this work, future studies should investigate how an optimised arrival time strategy combines with a weather routing system for ships with wind propulsion.

The optimisation parameters are also constrained to facilitate realistic and navigable routes, as the model limits the spatial movement of the ship to a maximum of seven closest grid points when travelling between each stage.

Furthermore, the wind-assisted ship propulsion (WASP) model sets a maximum engine power limit of 9.5 MW, which activates when the ship cannot achieve a given speed in adverse weather conditions. The VOIDS weather routing model filters any voyages that breach this maximum engine power limit.

Finally, weather-related safety constraints are not included in this study. Typically, when encountering a weather-related safety constraint, a ship will change its route or slow down to avoid adverse weather, which ensures safe navigation. While these situations occur in practice, Larsson and Simonsen (2014) find that the IMO proposed recommendations for the avoidance of potentially detrimental situations (IMO, 2007) are breached rarely and only in the most adverse weather conditions. As this study simulates thousands of departures, weather-related safety constraints will not significantly influence the results. Moreover, this analysis aims to investigate the influence of the stochastic behaviour of this wind. Including weather constraints will not influence this behaviour, and they are therefore excluded.

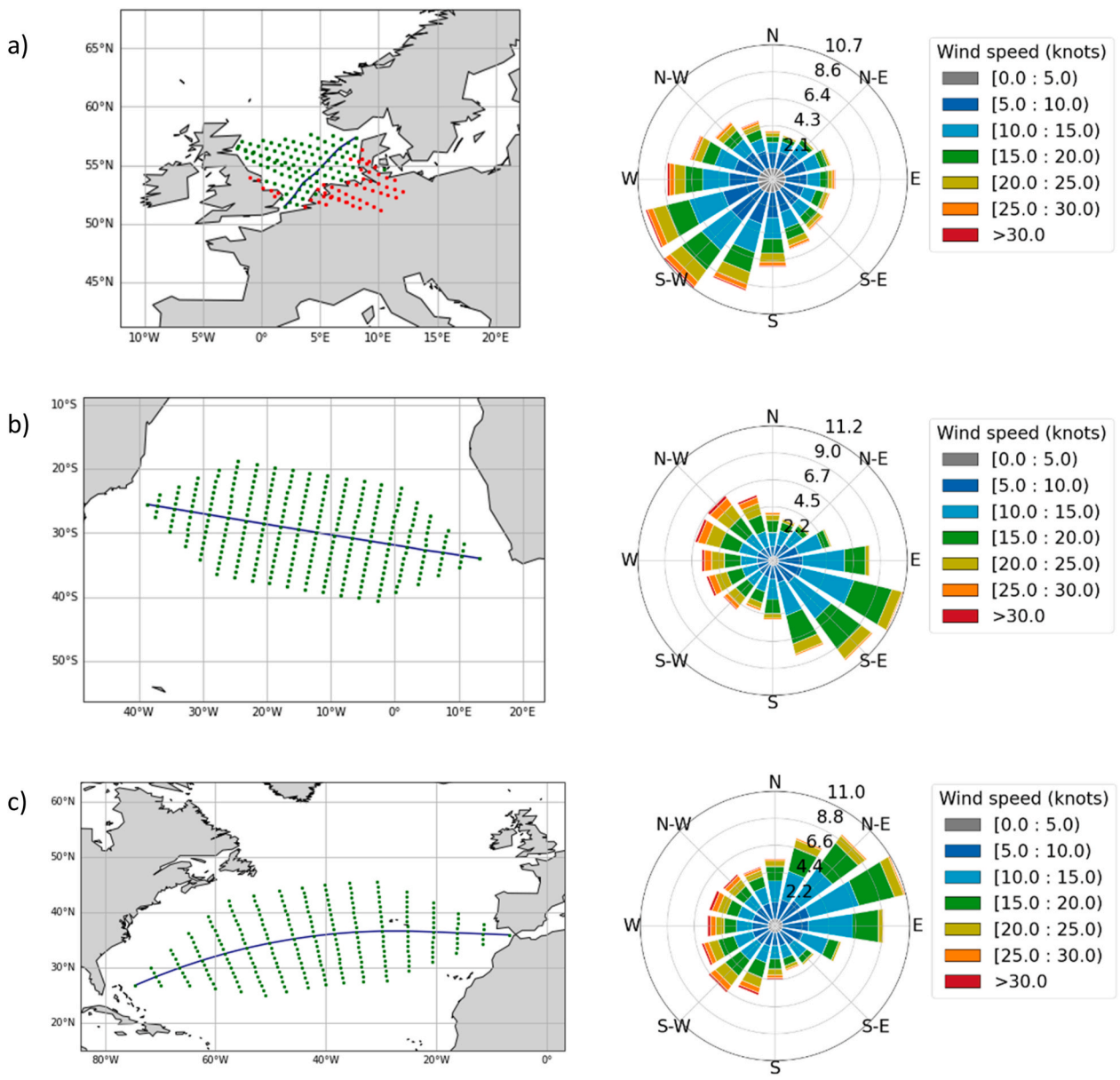

Fig. 3. A map of the automatic identification system (AIS) generated shipping route (blue line) and spatial graph points for the three case study routes in the North Sea (a), South Atlantic Ocean (b) and North Atlantic Ocean (c). Red points indicate filtered graph points, while the green points form the sailable region. Wind rose maps are also shown, depicting the wind speeds and wind angles in 2018, 2019 and 2020 in the Earth reference frame.

4. Case studies

4.1. Routes

To understand the impact of stochastic uncertainty on routes with different voyage times and wind profiles, eastbound and westbound journeys for three case study routes that represent contrasting route lengths are investigated. As the uncertainty in weather forecasts increases for predictions further into the future, this facilitates insights into this potentially key variable. The routes span different areas of the globe, including the South Atlantic Ocean, North Atlantic Ocean and North Sea (Fig. 3), and vary in total length from between 771 and 6400 km (Table 1). This corresponds to a total journey time of between 1.5 and 12.1 days.

All three great circle routes are generated using automatic identification system (AIS) ship data. However, as the computation time of weather routing simulations increases exponentially with grid size, the VOIDS model adapts the stage distance for each route, which varies between 65 and 400 km. Up to twenty perpendicular waypoints are generated for each stage to create the spatial graph, increasing in increments of four waypoints from the departure point and decreasing in increments of four waypoints to the arrival point, which forms the optimisation search space (Fig. 3). The distance between perpendicular waypoints is 50 km on Route 1 and 100 km on Routes 2 and 3. Route 1 requires a finer grid due to the smaller total voyage length.

The three case study routes also represent contrasting wind characteristics (Fig. 3). Route 1 experiences westerly winds with an average wind speed of 11.9 knots (Table 1). Route 2 experiences an amalgamation of light south-easterly trade winds to the north, alongside strong westerlies to the south, with an average wind speed of 14.2 knots. Finally, Route 3 experiences light north-easterly trade winds to the south, alongside strong westerlies to the north, with an average wind speed of 13.4 knots. Ultimately, wind characteristics are a particularly important factor for ships with wind propulsion, as Mason (2021) show that the carbon savings from Flettner rotors with and without weather routing vary from 4% to over 30% across fourteen global routes. The

Table 1
Route characteristics for the three case study routes investigated.

Area	Route 1	Route 2	Route 3
	North Sea	South Atlantic	North Atlantic
Departure destination	Denmark	South Africa	The Caribbean
Departure point	(57.4°N, 8.05°E)	(34.0°S, 13.3°E)	(26.8°N, 74.5°W)
Arrival destination	The UK	Brazil	Gibraltar
Arrival point	(51.4°N, 1.95°E)	(25.5°S, 38.7°W)	(35.9°N, 6.80°W)
Total distance (km)	771	5100	6400
Average stage distance (km)	64.3	268	399
Number of stages (waypoints)	12	19	16
Total voyage time (days)	1.46	9.23	12.1
Average speed (knots)	11.9	12.4	11.9
Perpendicular grid distance (km)	50	100	100
Average wind speed (knots)	11.9	14.2	13.4

prevailing wind speed and wind angle profiles of these routes are found to be the two dominant factors in this variation in performance. Therefore, the novel and contrasting nature of the wind profiles on both the eastbound and westbound journeys of these routes allow this analysis to additionally understand how wind characteristics impact stochastic uncertainty for weather routing.

4.2. Departure dates

A departure is simulated every 6 days from the start of each month for 2018, 2019 and 2020, generating a total of 180 departure date simulations. Each route is then simulated on the eastbound and westbound journey, forming a total of 1080 simulations. This accounts for the variable nature of weather conditions to facilitate statistically significant conclusions surrounding the annual propulsion performance of the technology when used as a carbon mitigation tool.

4.3. High-performance computer simulations

Due to the computationally intensive nature of the optimisation algorithm developed in this study, here we split the simulations into batches and run each batch simultaneously on a high-performance computer. The simulations are separated into individual departure dates, and on each, the forecast and realised carbon savings are calculated from wind propulsion on the great circle route, a priori optimum and adaptive optimum. The high-performance computer comprises high memory nodes of 32 GB RAM, with around 60 nodes available simultaneously. As each departure simulation has an average computation time of 2.6 h, this reduces the total computation time from 118 days to around 2 days for the 1080 total departure simulations.

5. Quantifying uncertainty in a priori weather routing strategies

A priori optimisation strategies in vehicle routing problems use information that is available at the start of the journey only (Manseur et al., 2018). For ships, an a priori strategy calculates optimum voyages using weather forecast data that is available when the ship initially leaves its departure point. On long shipping routes, a priori strategies can therefore calculate optimal voyages that are based on uncertain weather forecast predictions many days into the future. If weather conditions deviate from the predictions, fuel savings on the optimal voyage could reduce from the estimated value.

In real-time, ship operators do not use a priori methods, but update the forecasts as they travel deeper into their journey. Although a priori strategies are not used in practice, all studies in the weather routing literature for ships with wind propulsion implement this method (Ueno et al., 2004; Marie and Courteille, 2014; Yoshimura et al., 2016). As a priori strategies ignore forecast uncertainty, this study quantifies the strategy's sensitivity to stochastic wind forecasts to understand if the estimated carbon savings are achievable in practice.

5.1. Weather data

Here, we integrate three types of wind data into the VOIDS model to quantify the strategy's sensitivity to forecast uncertainty: 1) wind forecast data available at the start of the ship's journey, 2) historical reanalysis wind data and 3) ensemble wind forecast data. Fig. 4 shows an overview of how these data types are incorporated into the strategy's workflow.

5.1.1. Forecast wind data

First, the VOIDS weather routing model calculates an optimal voyage using the wind forecast available at the start of the ship's voyage. This voyage is termed the forecast optimum. Here, wind data is obtained from The Observing System Research and Predictability Experiment's (THORPEX) control forecast from the TIGGE dataset (Bougeault et al., 2010), which contains data with a $1^\circ \times 1^\circ$ spatial resolution and a 6-h time resolution for a total forecast prediction time of 360 h. Carbon savings of the wind-assisted ship on the forecast-optimum (FO) voyage, ΔE_{FO}, relative to the reference ship (R) on the great circle route, are calculated using:

$$\Delta E_{FO} = \frac{FC_R - FC_{FO}}{FC_R} \tag{5}$$

5.1.2. Reanalysis wind data

Second, the forecast-optimum's route and speed profile is retracked using reanalysis wind data. Here, reanalysis wind data is obtained from ECMWF's ERA5 dataset with a $1^\circ \times 1^\circ$ spatial resolution and a 6-h time resolution. This retracked route represents the weather and fuel consumption that the ship realises in practice and is termed here the realised forecast optimum. Carbon savings of the wind-assisted ship on the realised forecast optimum ($FO_{realised}$) voyage, $\Delta E_{FO_{realised}}$, are calculated using:

$$\Delta E_{FO_{realised}} = \frac{FC_R - FC_{FO_{realised}}}{FC_R} \tag{6}$$

The difference in carbon savings between the forecast optimum and the realised forecast optimum represents the impact of stochastic weather uncertainty for a priori optimal routing decisions for ships with wind propulsion.

5.1.3. Ensemble forecast wind data

Finally, the VOIDS model integrates ensemble forecast wind data to quantify the potential risk from the weather conditions changing as the ship progresses along its voyage (Hoffschildt et al., 1999). Rather than estimating one deterministic value, ensemble data accounts for the small error at the start of the weather forecast prediction to generate many ensemble members that each describe one scenario of how the weather may change in the future. Each ensemble member is equally likely to occur, and the spread of the ensemble members characterises the uncertainty of the forecast. This analysis uses fifty ensemble members from THORPEX's TIGGE dataset, with a $1^\circ \times 1^\circ$ spatial resolution and a 6-h time resolution. Fifty members represent the maximum number of ensembles offered by ECMWF and is larger than the number that other studies use in the weather routing literature for ships with wind propulsion (Yoshimura et al., 2016). Furthermore, this is the maximum number of members used in the standard ship routing literature (Hinnethal and Clauss, 2010; Skoglund et al., 2015; Vettor et al., 2021) and in yacht-routing studies (Treby, 2002; Kristensen, 2010). The forecast-optimum voyage is retracked with all 50 ensemble members to calculate the potential spread in fuel savings when combining weather routing with wind propulsion.

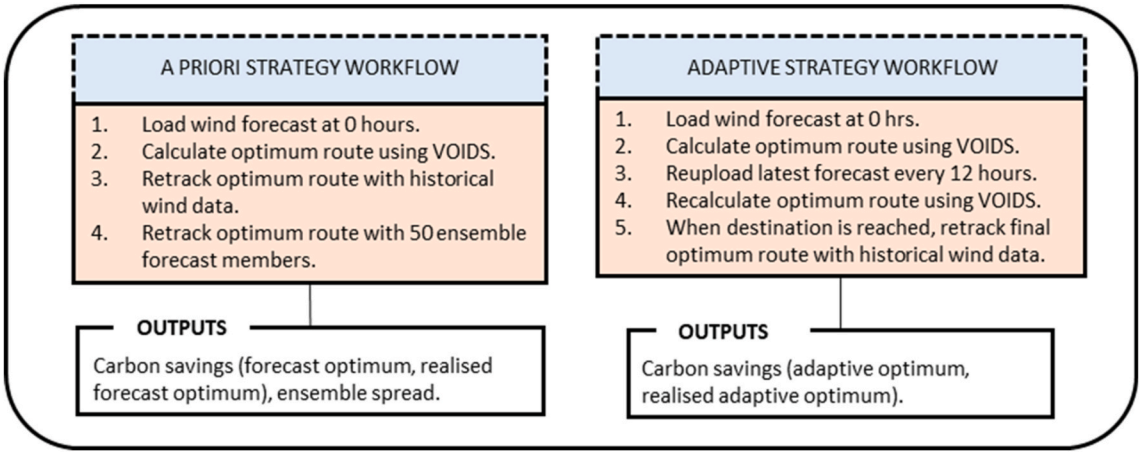

Fig. 4. An overview of the workflows for the a priori and adaptive strategies used in this study.

5.2. Uncertainty in wind forecasts

Fig. 5 shows an example of the fuel consumption of the wind-assisted ship when calculated with all three wind data types. The variation in fuel consumption along the journey can be substantial, and carbon savings from the ensemble members range from a maximum of 93.4% to a minimum of −18.1% across all departure dates. The large spread agrees with findings from Yoshimura et al. (2016), who find a similarly large ensemble range of between 92% and 32%. The ensemble minimum is greater than that found here, as Yoshimura et al. (2016) only simulate a wind ship for one departure date. The large range highlights the potential for the wind to change as the ship travels along its route, fostering uncertainty in the fuel consumption that the ship realises in practice. Moreover, and as expected, the induced uncertainty from the forecast increases over time, and retracking with ensemble data can identify the point at which the uncertainty starts to increase substantially for specific departures.

While the winds on some departures demonstrate high uncertainty, investigating all 180 departure dates provides statistically significant results (Fig. 6). As the weather routing software optimises the ship's voyage for one specific wind forecast, the estimated fuel consumption on this voyage is lower than the ensemble mean. This highlights a critical risk in a priori weather routing; if the weather changes and follows any other trajectory described by the ensemble spread, the realised fuel consumption on the optimum route will likely increase. This can reduce the potential carbon benefits of weather routing for ships with wind propulsion, particularly on routes that observe large carbon savings from the technology. On some departures, wind on the optimum route can change favourably for the ship and carbon savings increase relative to the predicted value. However, as the ship's fuel consumption averaged across all 180 departures is lower than the ensemble mean (Fig. 6), fuel consumption is more likely to increase, subsequently reducing carbon savings.

5.3. Carbon savings: forecast estimates vs realised savings

Averaging the carbon savings across all departures provides insights into the annual performance of the sails (Fig. 7). On the routes analysed here, we show that four Flettner rotors on a Panamax bulk carrier cut annual carbon emissions by 6.95%–16.7% on standard great circle routes. This agrees with other studies in the literature that investigate Flettner rotors for a similar ship type. Ammar and Seddiek (2022) find that four Flettner rotors reduce fuel use of a Panamax bulk carrier by 8.5%–16.2% on three case study routes, while Tillig and Ringsberg (2020) find that four Flettner rotors on a smaller tanker save over 25% on routes in the Pacific Ocean and Baltic Sea with beneficial winds.

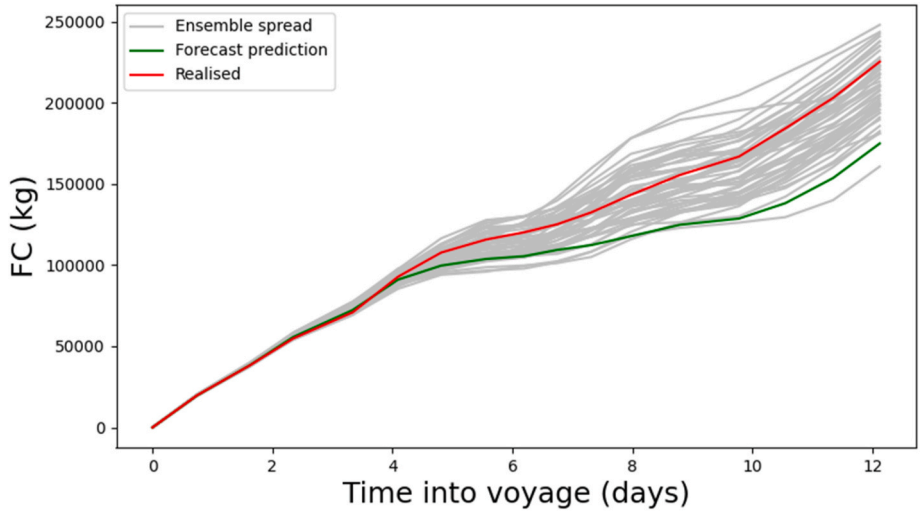

Fig. 5. Fuel consumption (FC) of the wind-assisted ship along the eastbound journey of Route 3 between the Caribbean and Gibraltar when using weather routing for a departure on February 7, 2018. The fuel consumption of the forecast-optimum route (green), the realised fuel consumption (red) and the spread in fuel consumption when retracking the fuel-optimised route with ensemble data (grey) are all shown.

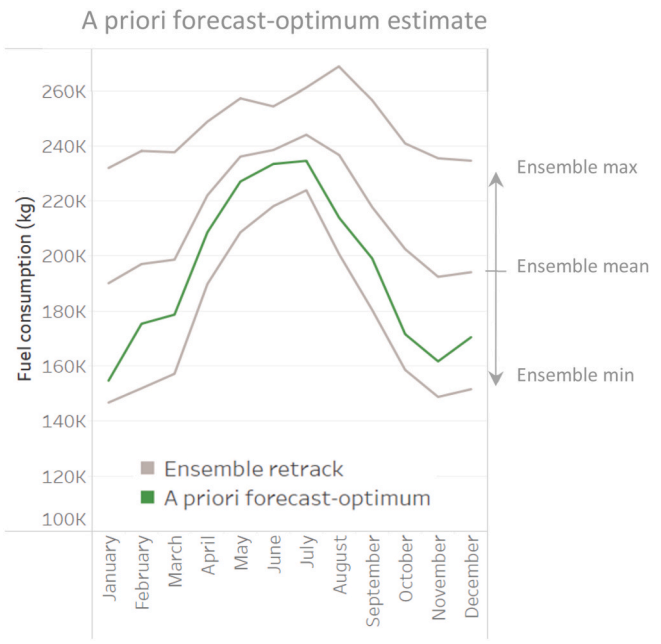

Fig. 6. Monthly averaged fuel consumption of the wind-assisted ship on the a priori forecast optimum voyage of Route 3 travelling in the eastbound direction.

Introducing a priori weather routing increases estimated carbon savings from the Flettner rotors to 10.2%–28.7%, representing a 1.17–2.81 times increase from the great circle route. Similarly, Bentin et al. (2016) find a 1.5–2.0 times increase when weather routing a ship with Flettner rotors, Yoshimura et al. (2016) demonstrate a 1.5 times increase and Zhang et al. (2013) find a 2.7 times increase. In this study, weather routing also increases the distance travelled by the ship by a maximum of 3.12% on average, while the arrival time limit in the VOIDS optimisation procedure constraints the voyage time of the ship, which decreases by less than 0.06%. Fig. 8 shows the carbon savings from the a priori strategy for each departure date. The savings display a large range between a maximum of 93.0% to a minimum of −9.62%, which highlights the Flettner rotor's critical dependency on the wind conditions experienced on each journey of operation. 6.85% of total departures on the great circle route generated negative savings across all routes, but this drops when using weather routing to 2.44% and 3.57% for the a priori forecast and realised routes respectively.

Weather routing optimises both the route and speed profile of the ship on all case study routes to produce these carbon savings (Fig. 9). The eastbound journeys of Routes 2 and 3 generate the largest benefits, as weather routing increases wind speeds and fine-tunes wind angles to tend towards the optimum angle for Flettner rotor sailing (Fig. 10), which occurs at around a southwest and southeast angle in the ship reference frame. Weather routing delivers less benefit on the westbound journeys of these routes but still generates notable savings, as optimisation reduces detrimental headwinds and partially increases ideal wind angles (see Supplementary Material). On Route 2 and Route 3, weather routing also delivers benefits from optimising ocean currents by increasing both the occurrence and strength of currents from behind the ship (Fig. 10 and Supplementary Material). Wind propulsion generates some of the largest great circle route savings on Route 1 due to the presence of beneficial wind angles, particularly on the eastbound journey (see Supplementary Material). This agrees with the findings of Mason (2021). However, the addition of weather routing produces less benefit on this route relative to Routes 2 and 3.

Retracking with historical weather data highlights the detrimental impact of stochastic uncertainty. The forecasted wind conditions change unfavourably to reduce the realised carbon savings across all routes (Fig. 7). Unfavourable wind changes have the greatest effect on the eastbound journey of Route 3, which has the longest journey, and carbon savings reduce from a theoretical 2.50 times increase to a realised 1.84 times increase, representing a 44% reduction in additional savings from the technology. Here, stochastic uncertainty in the initial wind forecast changes the realised wind conditions (Fig. 10), which reduces both the realised wind speeds and the occurrence of ideal wind angles.

This study is the first in the field to show that two dominant factors determine the influence of stochastic uncertainty across the routes analysed here. First, route length plays a key role, as the spread in uncertainty between the forecast and realised fuel consumption of the

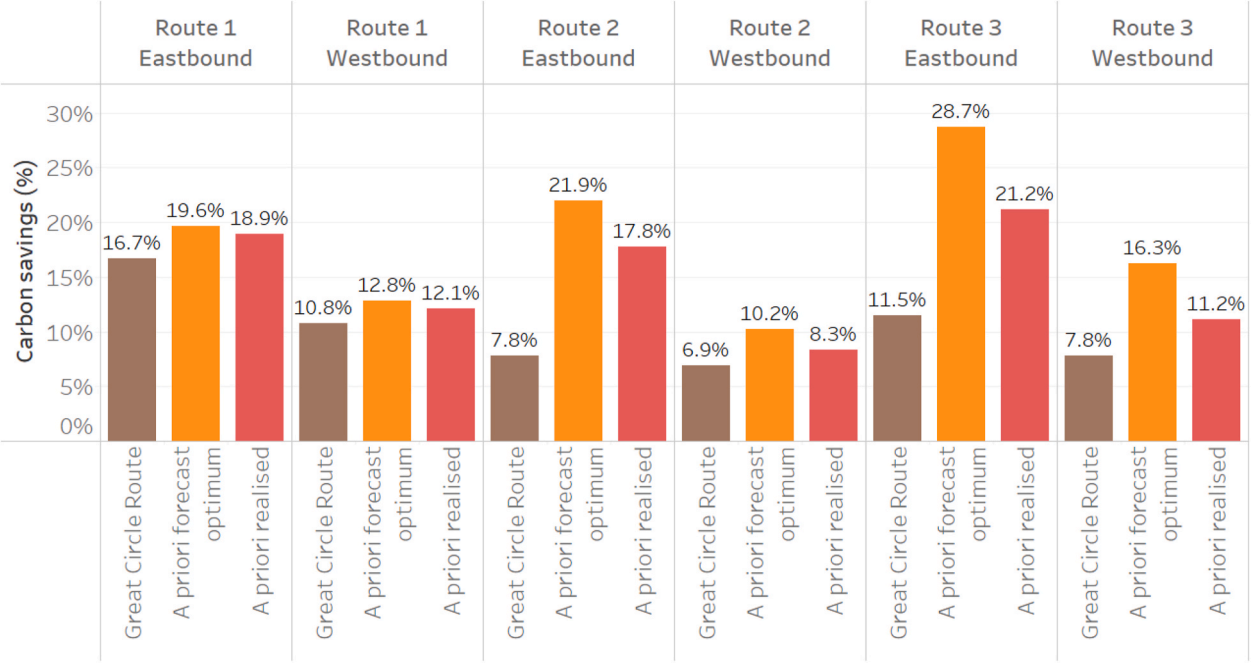

Fig. 7. Annual carbon savings from weather routing with wind propulsion when using the a priori strategy. Annual carbon savings on the great circle route (brown), the a priori forecast route (orange) and the a priori realised route (red) are shown.

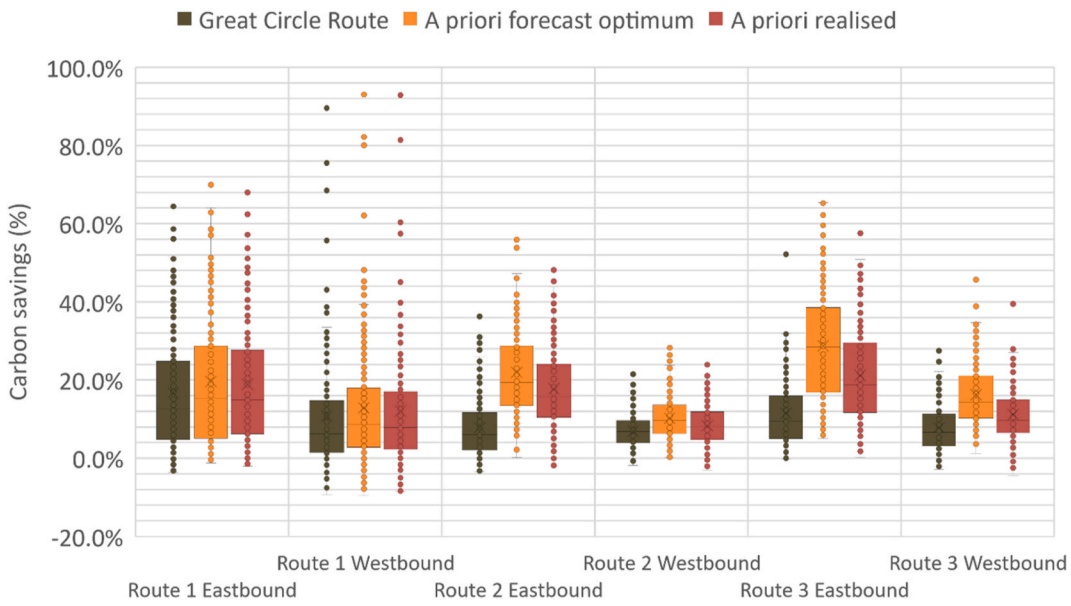

Fig. 8. A box and whisker plot showing the carbon savings from weather routing with wind propulsion using the a priori strategy on the routes assessed in this study. Each data point shows the carbon savings on each departure date for the great circle route (GCR) (brown), the a priori forecast route (orange) and the a priori realised route (red).

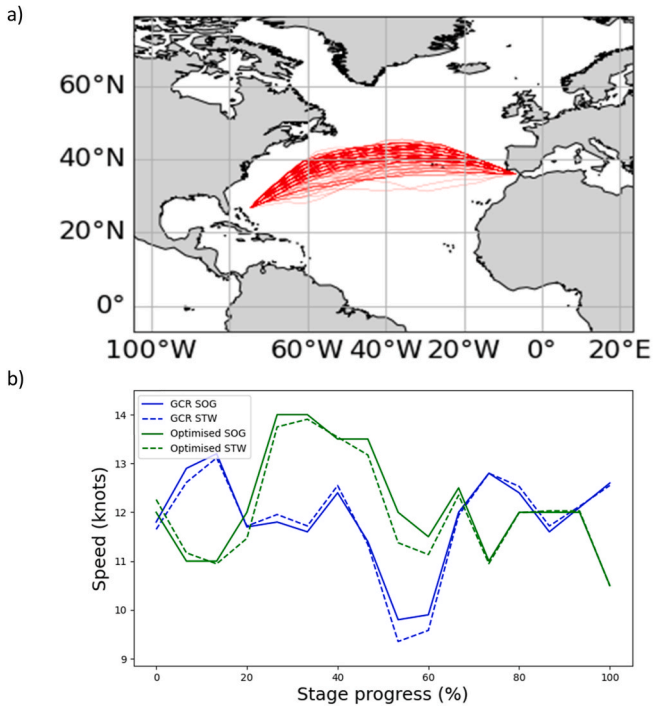

Fig. 9. Optimum routes for all 180 departures on the eastbound journey of Route 3 (a). Routes are calculated using a priori weather routing for a wind-assisted Panamax bulk carrier with four Flettner rotors. An example speed profile for the January 1, 2018 on the same route (b) showing both the speed over ground (SOG) (solid line) and speed through water (STW) (dashed line) on the great circle route (GCR) (blue) and optimised route (green).

wind-assisted ship increases over time across all 180 departures (Fig. 11). This is as expected, as weather forecast predictions become less accurate as time increases. This factor influences the findings here, as routes with a longer total voyage time experience greater uncertainty and, therefore, observe greater reductions in realised carbon savings (Fig. 7).

Second, the occurrence of high wind speeds at ideal angles for sailing influences the impact of stochastic uncertainty. The large impact at these specific wind conditions arises as Flettner rotor sails are most effective in this regime. Here, the sails can reduce the fuel consumption of the ship substantially. If the realised wind speed reduces or if the wind angle deviates from the ideal regime due to uncertain wind inputs, it can produce large and detrimental increases to the realised fuel consumption of the ship (Fig. 12). Therefore, optimum routes that produce savings by changing the wind regime to high wind speeds at ideal sail angles are most at risk from stochastic uncertainty. This occurs the most on the eastbound journeys of Route 2 and Route 3, which explains the larger reduction in carbon savings found on these routes. Similarly, departures that occur in higher wind speed winter months experience more uncertainty than in lower wind speed summer months due to the same effect.

Ultimately, the reduction in carbon savings from a priori weather routing found here challenges the suitability of existing optimisation methods in the wind-assist literature. While a priori methods are not used by ship operators in real time, questions remain around how achievable these theoretical savings are in practice. Results suggest that existing methods do not accurately predict the carbon savings that weather routing can realise in practice, particularly for longer shipping routes. However, while carbon savings reduce by some degree, a priori weather routing still provides benefits for ships with wind propulsion on the case study routes investigated, as the strength of wind speeds and the occurrence of ideal wind angles on the optimum route improve relative to standard routes. This result challenges other studies in the literature, as Rosander and Bloch (2000) find that high levels of forecast uncertainty remove all benefits of a priori weather routing for wind-assisted ships, reducing the carbon savings from weather routing with their novel sail design from 21.3% to −6.5%. Recent advances in wind forecast predictions are therefore sufficient to reduce uncertainty to a level that provides some carbon benefits. However, more advanced methods may be required to realise the theoretically maximum carbon savings from the technology.

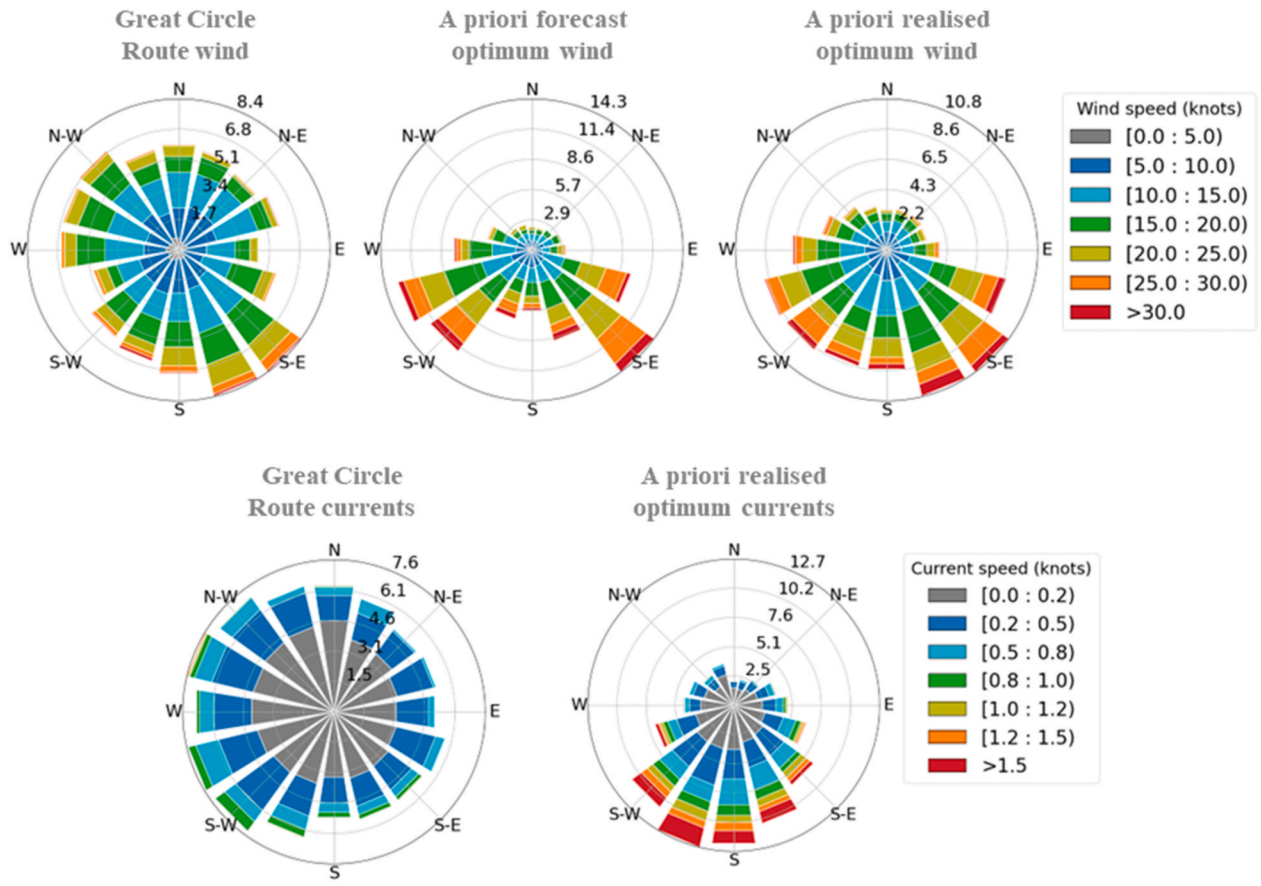

Fig. 10. Wind and current rose diagrams for the eastbound journey of Route 3 showing the wind speed and wind angle experienced by the ship on the great circle route (GCR) a priori forecast optimum and a priori realised optimum across all 180 departures. Wind angle is shown in the reference from of the ship, where north represents headwind and south represents tailwind.

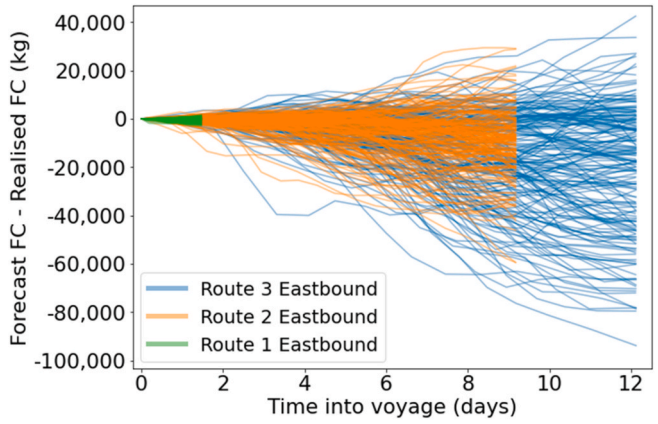

Fig. 11. The cumulative difference in the forecast and realised fuel consumption (FC) in kg estimated using the a priori optimisation strategy for all 180 departures on the eastbound journey of Routes 1, 2 and 3. The difference represents the discrepancy between the estimated fuel consumption and the fuel consumption realised in practice, where a negative value indicates a larger amount of fuel consumed in practice than initially estimated.

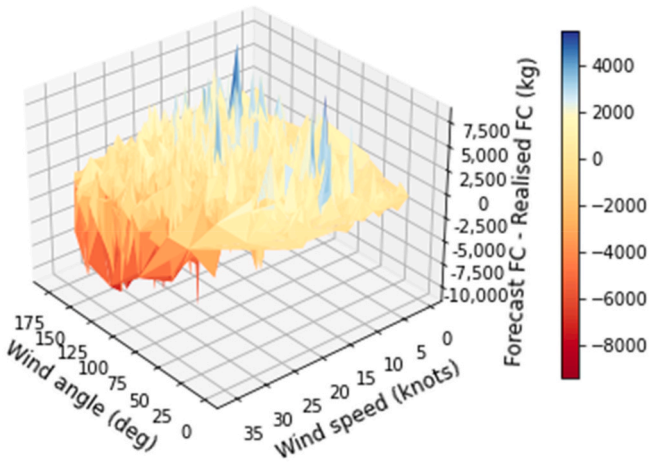

Fig. 12. A three-dimensional projection of how the forecasted wind speed and wind angle affects the difference in the forecast and realised fuel consumption (FC) in kg between each stage. The figure is estimated using the a priori optimisation strategy for all 180 departures on the eastbound journey of Route 2. Red indicates that the ship consumes a large amount of fuel in reality relative to the forecast prediction as it travels between a stage, while blue indicates that the ship consumes less fuel than the forecast prediction.

6. Reducing stochastic uncertainty: an adaptive optimisation strategy

This study develops an adaptive optimisation strategy, which is the standard routing procedure for ships in real-time, to understand if existing strategies can reduce the impact of forecast uncertainty when wind-assisted ships use weather routing. This provides insights into whether the theoretical a priori savings estimated in the literature are achievable in practice or whether they represent idealised values.

Adaptive optimisation strategies in vehicle routing problems adapt

the optimum solution based on information that becomes available along a journey (Manseur et al., 2018). In the same way, here the VOIDS weather routing model develops an adaptive strategy by uploading new wind forecast data in 12-h intervals as the ship moves along its voyage. This continually updates the optimisation procedure with the latest weather forecasts to reduce the influence of uncertain and stochastic weather forecast inputs. The following sections describe how the weather data is integrated into the model to achieve this aim, alongside a discussion of the results.

6.1. Weather data

6.1.1. Forecast updates

An overview of the adaptive strategy's workflow can be seen in Fig. 4. In this adaptive method, the VOIDS weather routing model first calculates an optimum voyage using the wind forecast available at the start of the journey. Here, the adaptive method again uses the control forecast from the TIGGE dataset from THORPEX. The data has a $1^\circ \times 1^\circ$ spatial resolution and a 6-h time resolution for a total forecast prediction time of 360 h. The ship then moves along this optimum route and speed path until the voyage time exceeds the 12-h upload increment. Once this time is exceeded and new weather forecast data is available for the ship operators to use, the VOIDS model uploads the latest TIGGE control forecast. Here, a new great circle route is generated using the average stage distance to split the route into a total of N_T stages and $N_T + 1$ total waypoints. The longitude and latitude of each great circle route waypoint are calculated using a method based on rotational transformation developed by Chen et al. (2015).

Once the VOIDS model has created an updated great circle route and has uploaded the latest wind forecast data, the model reruns the optimal voyage calculations with the position of the latest node as the starting point. This procedure recursively iterates every 12 h until the ship's destination point is reached. A retracking algorithm then retracks the optimal adaptive voyage, which is termed here as the adaptive optimum (AO), and the estimated fuel savings, ΔE_{AO}, are calculated using:

$$\Delta E_{AO} = \frac{FC_R - FC_{AO}}{FC_R} \tag{7}$$

As the adaptive optimisation strategy progresses, the total voyage time and graph size reduce for each new weather routing simulation. Therefore, this analysis updates the local optimisation strategy to maintain the computation time to around 15 min for each run. This facilitates a dense search space for the optimisation algorithm for each simulation. However, as the adaptive optimisation strategy requires additional runs of the optimisation algorithm in its recursive procedure, the total computation time of the strategy increases by around a factor of four relative to standard a priori strategies.

6.1.2. Reanalysis retrack

The adaptive optimum is retracked with ECMWF's ERA5 reanalysis wind data. This retracked voyage represents the weather and fuel consumption that the ship realises in practice and is termed here as the realised adaptive optimum ($AO_{realised}$). Carbon savings of the wind-assisted ship on the realised adaptive optimum voyage, ΔE_{RAO}, are calculated using:

$$\Delta E_{AO_{realised}} = \frac{FC_R - FC_{AO_{realised}}}{FC_R} \tag{8}$$

The difference in carbon savings between the adaptive optimum and the realised adaptive optimum represents the impact of stochastic weather uncertainty for adaptive optimal routing decisions for ships with wind propulsion.

6.2. Carbon savings: forecast estimates vs realised savings

Results show that optimum voyages calculated using an adaptive optimisation strategy accurately reflect the realised performance of weather routing technology on all case study routes investigated (Fig. 13). By uploading the most recent and accurate wind forecasts in 12-h intervals, adaptive optimisation reduces the discrepancies between the forecast and realised wind speed and wind angle data as the ship travels along its route. This more accurately aligns the ship's predicted fuel consumption with the fuel consumption realised in practice relative to the a priori strategy (Fig. 14).

The adaptive strategy has the greatest impact on the eastbound journey of Route 3, which previously displayed the largest risk from uncertain weather due to it having the longest 12-day voyage time. By investigating all 180 departure dates, we show that this translates to a substantially reduced spread in the difference between the ship's forecast and realised cumulative fuel consumption (Fig. 15). Ultimately, this reduced spread enables the adaptive optimum voyage to be more robust to stochastic changes in uncertain wind inputs.

As the adaptive strategy is part of standard routing procedures in the shipping sector, this result suggests that existing methods are suitable to reduce stochastic uncertainty for ships with wind propulsion. However, current practices may present a critical barrier, as optimum route calculations are typically rerun based on the user's judgement onboard the ship, which creates additional work for ship operators. As ships with wind propulsion are more susceptible to the impacts of uncertainty in wind forecasts, users may need to update weather forecasts more frequently than for standard ships, which occur around once per day. Failing to do so could detrimentally reduce the effectiveness of the adaptive strategy. Therefore, further work is necessary to understand the relationship between the forecast upload interval and the level of accuracy between estimated and realised carbon savings for ships with wind propulsion.

While the adaptive strategy reduces the risk from unfavourable changes to uncertain wind forecasts, the strategy detrimentally reduces the overall performance of the technology relative to a priori estimates. The adaptive optimal route is more robust to changes in wind, but the strategy fails to find the true global optimum solution, as forecast uncertainty alters the wind conditions in the optimisation search space leading to less-optimal results as the strategy iterates. When comparing the a priori forecast optimum (orange bar in Fig. 7), which contains no uncertainty, with the realised adaptive optimum (red bar in Fig. 13), the addition of uncertainty contributes to a reduction in the performance of weather routing by 0.794–0.879 times the maximum potential of the technology for Routes 2 and 3, the two longest routes analysed here. However, the shortest Route 1 reduces by only 0.983 to 1.00 times, achieving the maximum potential due to the shorter route length. For routes that are particularly sensitive to stochastic uncertainty, these results suggest that existing real-time weather routing methods are not suitable to achieve the maximum potential of the technology highlighted in a priori methods in the literature.

Although carbon savings reduce for longer route lengths relative to the maximum potential, the adaptive strategy amplifies the performance of the Flettner rotors significantly by between 1.16 and 2.48 times standard shipping routes. This challenges the conclusions from Rosander and Bloch (2000), who present the only other adaptive strategy for ships with wind propulsion and find that uncertain wind forecasts reduce the benefits from weather routing software enough to remove all motivation to use the technology. This suggests that advances in the accuracy of wind forecast predictions over the last two decades have directly reduced uncertainty from the combination of technologies studied here.

7. Limitations

Findings in this study show large uncertainty when wind-assisted ships use a priori weather routing. While carbon savings reduce by up to 44% using this method, weather routing is calculated here using a generic a priori route planning method. More advanced methods exist in the ship routing literature that are specifically designed to handle

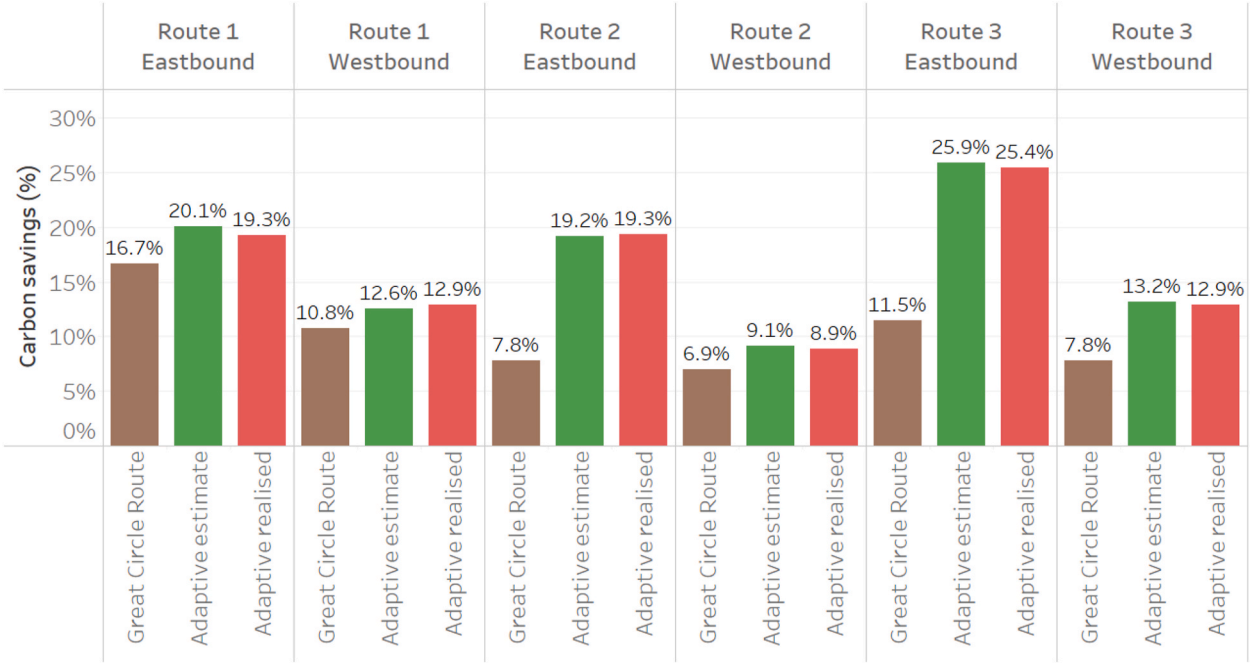

Fig. 13. The forecast (green) and realised (red) annual carbon savings from weather routing with wind propulsion achieved on all routes using the adaptive optimisation strategy. Carbon savings on the great circle route (GCR) (brown) are shown for reference.

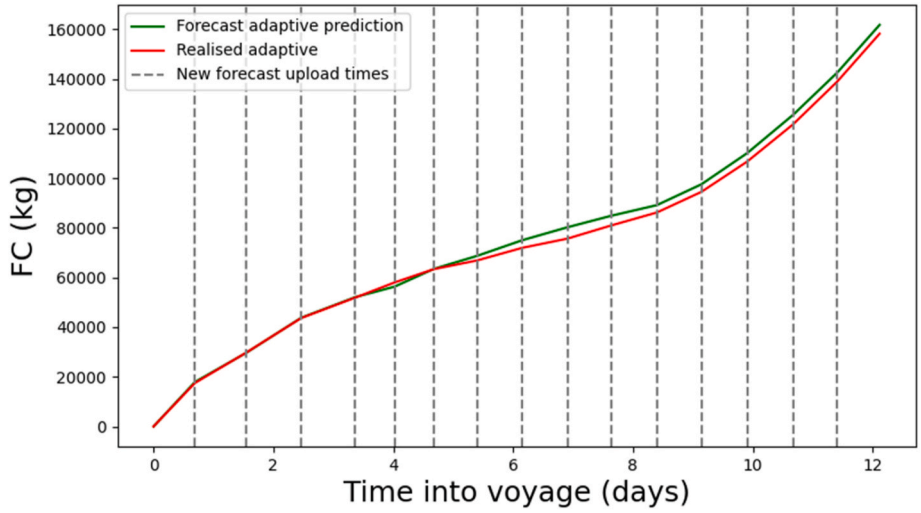

Fig. 14. The forecast (green) and achieved (red) fuel consumption (FC) of the wind-assisted Panamax bulk carrier ship on the adaptive optimum voyage for a departure on the January 1, 2018 on the eastbound journey of Route 3. New forecast upload times (grey) are shown to demonstrate when the adaptive optimisation strategy reuploads the latest wind forecast data and reruns the weather routing algorithm.

uncertainty, such as by including ensemble weather forecasts in the optimisation procedure. Vettor et al. (2020) describe one such approach, where the optimisation algorithm handles all ensemble members in a single run. Here, the fuel consumption of the ship can be calculated for all ensemble members at each route waypoint and could only be considered safe if the spread is suitably small. Hinnethal and Clauss (2010) develop a method that integrates ensemble forecasts to calculate the robustness of a route, where a route is considered robust if it doesn't breach specified constraints across many ensemble members. Similarly, other studies in the wider field of vehicle routing use ensemble forecasts to handle uncertainty by calculating the expected value of the members at each waypoint (Sheng and Mei, 2020; Gendreau et al., 2015; Huang and Gao, 2012).

Including ensemble members in the optimisation procedure would increase computation time substantially and is therefore not a suitable solution for this study due to the prohibitive number of departures analysed. However, integrating these methods into the field of ship routing for wind-assisted ships would likely reduce the discrepancy found in this paper between expected and achieved carbon savings and should be considered an important area of future research. While existing studies present viable methods, effectively handling uncertainty while simultaneously maximising the performance of the sails may present a more challenging problem than in other fields. Existing methods, in particular those surrounding robustness, would likely calculate solutions with carbon savings that are more achievable in practice, but may compromise the strength of the optimal solution leading to lower carbon savings overall. In this regard, Philpott and Mason (2001) criticise the existing form of ensemble weather data and

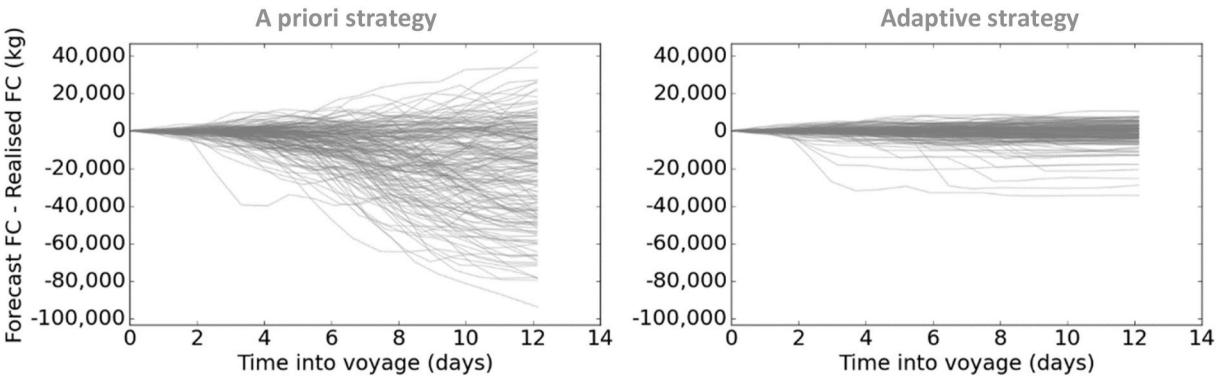

Fig. 15. The difference in the forecast and realised cumulative fuel consumption (FC) in kg estimated using the a priori and adaptive optimisation strategy for all 180 departures on the eastbound journey of Route 3. The difference represents the discrepancy between the estimated fuel consumption and the fuel consumption realised in practice, where a negative value indicates a larger amount of fuel consumed in practice than initially estimated.

show that a new structure for ensemble forecasts would be more suitable to this challenge. Rather than forming fifty individual ensemble branches, this new structure creates sub-branches within the individual members, which provides the optimisation algorithm with more information as the ship travels along its journey. However, this form of ensemble data does not currently exist.

Finally, the conclusions drawn here are for Panamax bulk carrier ships with Flettner rotors. Other ship types, sail types and sail configurations could change these results. In particular, ships with fewer or smaller rotors would produce less sail power and would therefore experience less impact from stochastic wind forecasts, as the ship becomes less dependent on the wind. Findings may also change for different sail types, such as wing sails, which demonstrate a different performance profile to Flettner rotors.

8. Conclusion

This study provides new insights into the stochastic variability of wind forecasts when weather routing technology amplifies the carbon savings from ships with wind propulsion. By running over 1000 simulated departures across three routes using multiple weather data types, we produce the first statistically robust assessment to show that stochastic uncertainty can substantially reduce the benefits of a priori weather routing by up to 44% on particularly impacted routes. This result challenges both the accuracy and suitability of the weather routing methods in the scientific literature when employed in real-time for ships with wind propulsion.

When a priori weather routing is exploited on different routes, stochastic uncertainty has the greatest impact when coupled with longer voyage times. Moreover, this study correlates fuel consumption uncertainty with wind speed and wind angle data from over a thousand departures to show that optimum routes that encounter high wind speeds and ideal wind angles simultaneously experience the greatest risk from forecast uncertainty. As the shipping sector requires urgent global action to reduce carbon emissions, this novel finding provides a deeper understanding of which routes may demand advanced optimisation methods to reduce forecast uncertainty and drive carbon savings closer to the theoretical estimates presented in the scientific literature.

Finally, by re-uploading new wind forecast data in 12-h intervals, this study finds that adaptive optimisation strategies can effectively mitigate stochastic uncertainty. The adaptive strategy not only calculates achievable optimal routes but also amplifies carbon savings from Flettner rotors substantially by between 1.16 and 2.48 times typical great circle route savings. While more advanced methods will be required to drive savings closer to the theoretical maximum on particularly impacted routes, weather routing systems can implement adaptive strategies to accurately estimate carbon savings for ships with wind propulsion and reduce the financial risk for ship operators and sail investors. Overall, as the shipping sector requires rapid action this decade to align emission trajectories with Paris-compliant objectives (Bullock et al., 2022), our findings provide the much-needed deeper understanding into the scale of carbon mitigation offered by combining wind propulsion with weather routing when stochastic uncertainty is addressed. Accounting for the impact of these real-time factors highlights the suitability of an alternative short-term decarbonisation strategy for shipping that complements long-term investment in alternative fuels.

CRediT authorship contribution statement

James Mason: Conceptualization, Methodology, Software, Validation, Formal analysis, Writing – original draft, Visualization, Project administration. **Alice Larkin:** Conceptualization, Writing – review & editing, Supervision, Funding acquisition. **Alejandro Gallego-Schmid:** Conceptualization, Writing – review & editing, Supervision, Project administration, Funding acquisition.

Declaration of competing interest

The authors declare that they have no known competing financial interests or personal relationships that could have appeared to influence the work reported in this paper.

Data availability

Data will be made available on request.

Acknowledgements

This work was supported by the Engineering and Physical Sciences Research Council's (EPSRC) Doctoral Prize Fellowship (J.M.).

This work is based on TIGGE data. TIGGE (The Interactive Grand Global Ensemble) is an initiative of the World Weather Research Programme (WWRP).

This work is based on ship performance data obtained from Blue Wasp Marine.

Appendix A. Supplementary data

Supplementary data to this article can be found online at https://doi.org/10.1016/j.oceaneng.2023.114674.

References

Ammar, N.R., Seddiek, I.S., 2022. Wind assisted propulsion system onboard ships: case study Flettner rotors. Ships Offshore Struct. 17 (7), 1616–1627. https://doi.org/10.1080/17445302.2021.1937797.

Ampah, J.D., Yusuf, A.A., Afrane, S., Jin, C., Liu, H., 2021. Reviewing two decades of cleaner alternative marine fuels: towards IMO's decarbonization of the maritime transport sector. J. Clean. Prod. 320.

Bellman, R., 1957. Dynamic Programming. Princeton University Press, Princeton, NJ.

Bordogna, G., Muggiasca, S., Giappino, S., Belloli, M., Keuning, J.A., Huijsmans, R.H.M., van't Veer, A.P., 2019. Experiments on a Flettner rotor at critical and supercritical Reynolds numbers. J. Wind Eng. Ind. Aerod. 188.

Bentin, M., Zastrau, D., Schlaak, M., Freye, D., Elsner, R., Kotzur, S., 2016. A New Routing Optimization Tool-influence of Wind and Waves on Fuel Consumption of Ships with and without Wind Assisted Ship Propulsion Systems. Transportation Research Procedia 14, 153–162. https://doi.org/10.1016/j.trpro.2016.05.051.

Bordogna, G., Muggiasca, S., Giappino, S., Belloli, M., Keuning, J.A., Huijsmans, R.H.M., 2020. The effects of the aerodynamic interaction on the performance of two Flettner rotors. J. Wind Eng. Ind. Aerod. 196.

Bougeault, P., Toth, Z., Bishop, C., Brown, B., Burridge, D., Chen, D.H., Ebert, B., Fuentes, M., Hamill, T.M., Mylne, K., Nicolau, J., Paccagnella, T., Park, Y.Y., Parsons, D., Raoult, B., Schuster, D., Dias, P.S., Swinbank, R., Takeuchi, Y., Tennant, W., Wilson, L., Worley, S., 2010. The THORPEX interactive Grand global ensemble. Bull. Am. Meteorol. Soc. 91, 1059–1072. https://doi.org/10.1175/2010BAMS2853.1.

Bullock, S., Mason, J., Broderick, J., Larkin, A., 2020. Shipping and the Paris climate agreement: a focus on committed emissions. BMC Energy 2.

Bullock, S., Mason, J., Larkin, A., 2022. The urgent case for stronger climate targets for international shipping. Clim. Pol.

Chen, C.-L., Hsieh, T.-H., Hsu, T.-P., 2015. A novel approach to solve the great circle sailings based on rotation transformation. J. Mar. Sci. Technol. 23, 13–20.

Deyemer, S., Audenaert, P., Pickavet, M., Demeester, P., 2013. Dynamic and stochastic routing for multimodal transportation systems. IET Intell. Transp. Syst. https://doi.org/10.1049/iet-its.2012.0065.

Dnv, G.L., 2018. Maritime Forecast to 2050 - Energy Transition Outlook 2018. https://eto.dnv.com/2018/maritime.

ECMWF, 2022. ERA5 Database. European Centre for Medium-Range Weather Forecasts (ECMWF). https://www.ecmwf.int/en/forecasts/datasets/reanalysis-datasets/era5.

ESR, 2009. OSCAR third degree resolution ocean surface currents database. In: Earth Space Research (ESR), Physical Oceanography Distributed Active Archive Center (PODAAC). https://doi.org/10.5067/OSCAR-03D01.

GEBCO, 2022. Gridded Bathymetry Data. General Bathymetric Chart of the Oceans (GEBCO). https://www.gebco.net/data_and_products/gridded_bathymetry_data/.

Gendreau, M., Ghiani, G., Guerriero, E., 2015. Time-dependent routing problems: a review. Comput. Oper. Res. 64, 189–197. https://doi.org/10.1016/j.cor.2015.06.001.

Gerritsma, J., Beukelman, W., 1972. Analysis of the resistance increase in waves of a fast cargo ship. Int. Shipbuild. Prog. 19, 285–293.

Hinnethal, J., Clauss, G., 2010. Robust Pareto-optimum routing of ships utilising deterministic and ensemble weather forecasts. Ships Offshore Struct. 5 (2), 105–144.

Hoffschildt, M., Bidlot, J.R., Hansen, B., Janssen, P.A.E.M., 1999. Potential Benefit of Ensemble Forecasts for Ship Routing. European Centre for Medium-Range Weather Forecasts (ECMWF). https://doi.org/10.21957/ucgxanos0.

Huang, H., Gao, S., 2012. Optimal paths in dynamic networks with dependent random link travel times. Transp. Res. Part B Methodol. 46 https://doi.org/10.1016/j.trb.2012.01.005.

IMO, 2007. MSC.1/Circ.1228 Revised Guidance to the Master for Avoiding Dangerous Situayions in Adverse Weather and Sea Conditions. https://wwwcdn.imo.org/localresources/en/OurWork/Safety/Documents/Stability/MSC.1-CIRC.1228.pdf.

IMO, 2014. Third IMO Greenhouse Gas Study 2014. International Maritime Organisation (IMO), London. https://greenvoyage2050.imo.org/wp-content/uploads/2021/01/third-imo-ghg-study-2014-executive-summary-and-final-report.pdf.

IMO, 2018. MEPC.304(72) Initial IMO Strategy on reduction of GHG emissions from ships. In: International Maritime Organisation (IMO). https://wwwcdn.imo.org/localresources/en/KnowledgeCentre/IndexofIMOResolutions/MEPCDocuments/MEPC.304(72).pdf.

IMO, 2020. Fourth IMO GHG Study 2020. International Maritime Organisation (IMO), London. https://greenvoyage2050.imo.org/wp-content/uploads/2021/07/Fourth-IMO-GHG-Study-2020-Full-report-and-annexes_compressed.pdf.

IMO, 2021. MEPC.1/Circ.896 2021 Guidance on Treatment of Innovative Energy Efficiency Technologies for Calculation and Verification of the Attained EEDI and EEXI. International Maritime Organisation (IMO), London. https://wwwcdn.imo.org/localresources/en/OurWork/Environment/Documents/Air pollution/MEPC.1-Circ.896.pdf.

IMO, 2022. MEPC 79/INF.21 Wind Propulsion. International Maritime Organisation (IMO), London. https://www.wind-ship.org/wp-content/uploads/2022/10/MEPC-79-INF.21-Wind-Propulsion-Finland-France-Saudi-Ar....pdf.

Kim, M., Hizir, O., Turan, O., Day, S., Incecik, 2017. A. Estimation of added resistance and ship speed loss in a seaway. Ocean Eng. 141.

Kristensen, N.M., 2010. Weather Routing: Sensitivity to Ensemble Wind and Current Input. Master's thesis, University of Oslo.

Larsson, E., Simonsen, M.H., 2014. DIRECT Weather Routing. MSc thesis, Chalmers University of Technology.

Lu, R., Turan, O., Boulougouris, E., Banks, C., Incecik, A., 2015. A semi-empirical ship operational performance prediction model for voyage optimization towards energy efficient shipping. Ocean Eng. 110.

Manseur, F., Nadir, F., Nguyen Van Phu, C., Haj-Salem, H., Lebacque, J.P., 2018. Robust routing, its price, and the tradeoff between routing robustness and travel time reliability in road networks. Eur. J. Oper. Res. 285 (1), 159–171.

Marie, S., Courteille, E., 2014. Sail-assisted motor vessels weather routing using a fuzzy logic model. J. Mar. Sci. Technol. 19, 265–279.

Mason, J., 2021. Quantifying Voyage Optimisation with Wind-Assisted Ship Propulsion: a New Climate Mitigation Strategy for Shipping. Doctoral thesis. The University of Manchester.

Merkel, A., Kalantari, J., Mubder, A., 2022. Port call optimization and CO2-emissions savings – estimating feasible potential in tramp shipping. Marit. Transport. Res. 3 https://doi.org/10.1016/j.martra.2022.100054.

Morgas, W., Kopacz, Z., 2013. Rhumb-line sailing by computation. Rep. Geodesy Geoinf. 94, 14–26. https://doi.org/10.2478/rgg-2013-0003.

NOAA, 2017. Global Self-Consistent, Hierarchical, High-Resolution Geography Database (GSHHG). National Oceanic and Atmospheric Administration (NOAA). https://www.ngdc.noaa.gov/mgg/shorelines/.

Philpott, A., Mason, A., 2001. Optimising yacht routes under uncertainty. In: SNAME 15th Chesapeake Sailing Yacht Symposium. https://doi.org/10.5957/CSYS-2001-009.

Pierson, W.J., Moskowitz, L., 1964. A proposed spectral form for fully developed wind seas based on the similarity theory of S. A. Kitaigorodskii. J. Geophys. Res. 69, 5181–5190.

Rosander, M., Bloch, J.O.V., 2000. Modern Windships. Knud E. Hansen. https://www2.mst.dk/udgiv/publications/2000/87-7944-019-3/pdf/87-7944-020-7.pdf.

Seddiek, I.S., Ammar, N.R., 2021. Harnessing wind energy on merchant ships: case study Flettner rotors onboard bulk carriers. Environ. Sci. Pollut. Res. 28, 32695–32707.

Sheng, Y., Mei, X., 2020. Uncertain random shortest path problem. Soft Comput. 24 https://doi.org/10.1007/s00500-018-03714-5.

Skoglund, L., Kuttenkeuler, J., Rosén, A., Ovegard, E., 2015. A comparative study of deterministic and ensemble weather forecasts for weather routing. J. Mar. Sci. Technol. 20, 429–441. https://doi.org/10.1007/s00773-014-0295-9.

Smith, T., Newton, P., Winn, G., La Rosa, A.G., 2013. Analysis Techniques for Evaluating the Fuel Savings Associated with Wind Assistance. Low Carbon Shipping 2013, London.

Tillig, F., Ringsberg, J., 2020. Design, operation and analysis of wind-assisted cargo ships. Ocean Engineering 211, 107603. https://doi.org/10.1016/j.oceaneng.2020.107603.

Traut, M., Gilbert, P., Walsh, C., Larkin, A., Filippone, A., Stansby, P.K., Wood, F., 2014. Propulsive power contribution of a kite and a Flettner rotor on selected shipping routes. Appl. Energy 113, 362–372.

Treby, A., 2002. Optimal weather routing using ensemble weather forecasts. In: Proceedings of the 37th Annual Conference. Operational Research Society of New Zealand.

Ueno, M., Tsujimoto, M., Kitamura, F., Fujiwara, T., Takekawa, M., Nakayama, K., Issiki, H., Fujita, H., Horooka, H., 2004. Fundamental Research for Development of an Advanced Sail-Assisted Ship, 2, pp. 1102–1109. https://doi.org/10.1109/OCEANS.2004.1405664.

van der Kolk, N.J., Keuning, J.A., Huijsmans, R.H.M., 2019. Part 1: experimental validation of a RANS-CFD methodology for the hydrodynamics of wind-assisted ships operating at leeway angles. Ocean Eng. 178.

van der Kolk, N.J., Akkerman, I., Keuning, J.A., Huijsmans, R.H.M., 2020. Part 2: simulation methodology and numerical uncertainty for RANS-CFD for the hydrodynamics of wind-assisted ships operating at leeway angles. Ocean Eng. 201.

Vettor, R., Szlapczynska, J., Szlapczynski, R., Tycholiz, W., Guedes Soares, C., 2020. Towards Improving Optimised Ship Weather Routing, 27. Polish Maritime Research, pp. 60–69. https://doi.org/10.2478/pomr-2020-0007.

Vettor, R., Bergamini, G., Guedes Soares, C., 2021. A comprehensive approach to account for weather uncertainties in ship route optimization. J. Mar. Sci. Eng. 9 (12), 1434. https://doi.org/10.3390/jmse9121434.

Wang, H., Mao, W., Eriksson, L., 2017. Benchmark study of five optimization algorithms for weather routing. In: Proceedings of the International Conference on Offshore Mechanics and Arctic Engineering.

Yoshimura, Y., Ouchi, K., Waseda, T., 2016. Contributions to EEOI and EEDI by Wind Challenger Ships. Advanced Maritime Engineering Conference (AMEC), 2016.

Zhang, Y., Yuankui, L., Xuefeng, Y., 2013. Route optimization algorithm for minimum fuel consumption of wind-assisted ship. Journal of Applied Sciences 13 (21), 4805–4811. https://doi.org/10.3923/jas.2013.4805.4811.